Article

Nitrate Adsorption and Reduction on Cu(100) in Acidic Solution

Sang-Eun Bae, Karen L. Stewart, and Andrew A. Gewirth

J. Am. Chem. Soc., **2007**, 129 (33), 10171-10180• DOI: 10.1021/ja071330n • Publication Date (Web): 27 July 2007

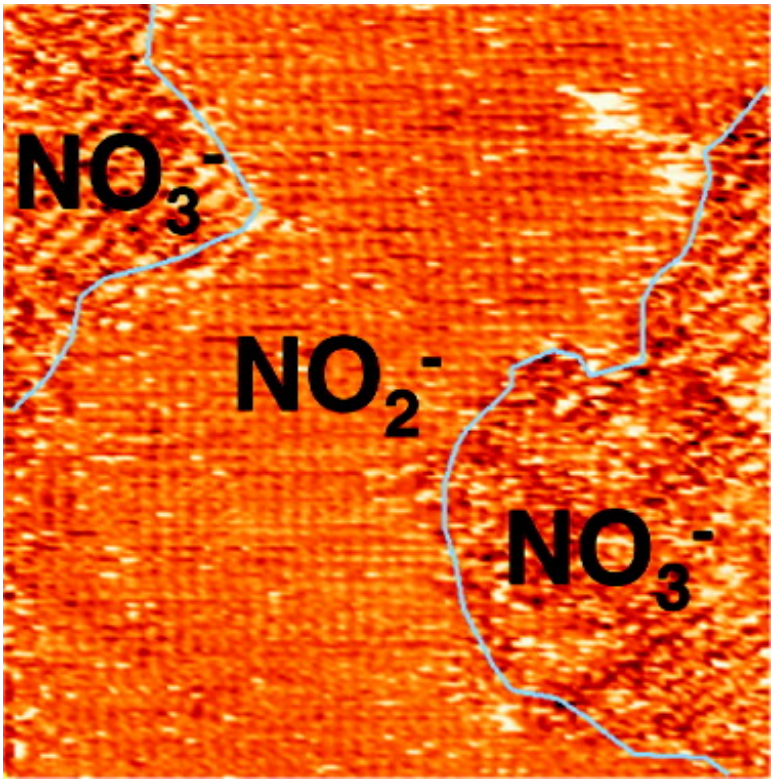

More About This Article

Additional resources and features associated with this article are available within the HTML version:

- Supporting Information
- Links to the 1 articles that cite this article, as of the time of this article download
- Access to high resolution figures
- Links to articles and content related to this article
- Copyright permission to reproduce figures and/or text from this article

J|A|C|S
ARTICLES
Published on Web 07/27/2007

Nitrate Adsorption and Reduction on Cu(100) in Acidic Solution

Sang-Eun Bae, Karen L. Stewart, and Andrew A. Gewirth*

Contribution from the Department of Chemistry, University of Illinois, Urbana, Illinois 61801

Received February 25, 2007; E-mail: agewirth@uiuc.edu

Abstract: Nitrate adsorption and reduction on Cu(100) in acidic solution is studied by electrochemical methods, in situ electrochemical scanning tunneling microscopy (EC-STM), surface enhanced Raman spectroscopy (SERS), and density functional theory (DFT) calculations. Electrochemical results show that reduction of nitrate starts at −0.3 V vs Ag/AgCl and reaches maximum value at −0.58 V. Over the entire potential region interrogated adlayers composed of nitrate, nitrite, or other intermediates are observed by using in situ STM. From the open-circuit potential (OCP) to −0.22 V vs Ag|AgCl, the nitrate ion is dominant and forms a (2 × 2) adlattice on the Cu(100) surface while nitrate forms a dominantly *c*(2 × 2) structure from −0.25 to −0.36 V. The interconversion between the nitrate and nitrite adlattices is observed. DFT calculations indicate that both nitrate and nitrite are twofold coordinated to the Cu(100) surface.

1. Introduction

The adsorption and reduction of nitrate at metal surfaces have long attracted considerable interest because of its environmental importance[1] and its putative role in the production of useful nitrato compounds.[2] Nitrate contamination of water must be remediated because of the deleterious effect of nitrate on human health and the environment.[1,3] Nitrate has also been a main starting material to produce useful nitrato compounds such as ammonia, hydroxylamine, hydrazine, and azides.[2,4] Nitrate electroreduction has been studied on several metal surfaces by using conventional electrochemical techniques,[1,5−7] FTIR,[8−10] Raman,[11] and mass[4] spectroscopic methods.

In aqueous media, nitrate electroreduction proceeds by several pathways depending on electrode composition and pH of the electrolytes.[4,12,13] One of the most active electrode materials for nitrate electroreduction is Cu.[4] In order to obtain better efficiency, a Cu alloy[8,14−16] or a modified Cu surface[1,7] has been employed. On many transition metal surfaces, including Pt and Rh, the predominate stable intermediate found during the electroreduction of nitrate to ammonia is adsorbed nitric oxide (NO).[17] However, on Cu the same reaction yields gaseous NO in acidic media[4] and a nitrite ion (NO_2^-) in alkaline solution.[13]

On copper surfaces, nitrate reduction in acidic media takes place through an eight-electron pathway, as shown in eq 1

$$NO_3^- + 8e^- + 9H^+ \rightarrow 3H_2O + NH_3 \qquad E^0 = 0.68 \text{ V vs Ag/AgCl} \quad (1)$$

On the basis of the observation of intermediates, it is thought that the reaction proceeds stepwise, through successively more reduced intermediates. The rate determining step (rds) for nitrate reduction is interrogated by using a Tafel slope, although of course a Tafel slope alone cannot specify a mechanism.[18] The Tafel slopes measured for nitrate electroreduction on many transition metal electrodes are found close to 120 mV/decade[4] which suggests that the first electron transfer, involving the reduction of nitrate to nitrite, is the rds. However, the Tafel slope measured on the Cu surface is somewhat larger than 120 mV/decade.[4] Additionally, the reduction of nitrite on Cu occurs at potentials less negative than those for the nitrate reduction.[7] There is little understanding concerning the intermediates involved in nitrate electroreduction on Cu or the relationship between the electroreduction event and nitrate and/or nitrite surface structure.

Among anions, halide ions and oxoanions are well-known to adsorb on fcc metal surfaces.[19] For example on the Cu(111) surface, chloride ion forms a $c(p \times \sqrt{3})$ adlattice while the

(1) Moorcroft, M. J.; Davis, J.; Compton, R. G. *Talanta* **2001**, *54*, 785−803.
(2) Plieth, W. F. *Encyclopedia of Electrochemistry of the Elements*; Marcel Dekker: New York, 1978.
(3) Reyter, D.; Chamoulaud, G.; Belanger, D.; Roue, L. *J. Electroanal. Chem.* **2006**, *596*, 13−24.
(4) Dima, G. E.; de Vooys, A. C. A.; Koper, M. T. M. *J. Electroanal. Chem.* **2003**, *554*, 15−23.
(5) Pletcher, D.; Poorabedi, Z. *Electrochim. Acta* **1979**, *24*, 1253−1256.
(6) Carpenter, N. G.; Pletcher, D. *Anal. Chim. Acta* **1995**, *317*, 287−293.
(7) Davis, J.; Moorcroft, M. J.; Wilkins, S. J.; Compton, R. G.; Cardosi, M. F. *Analyst* **2000**, *125*, 737−741.
(8) da Cunha, M.; De Souza, J. P. I.; Nart, F. C. *Langmuir* **2000**, *16*, 771−777.
(9) Moraes, I. R.; daCunha, M.; Nart, F. C. *J. Brazil. Chem. Soc.* **1996**, *7*, 453−460.
(10) daCunha, M.; Weber, M.; Nart, F. C. *J. Electroanal. Chem.* **1996**, *414*, 163−170.
(11) Castro, P. M.; Jagodzinski, P. W. *J. Phys. Chem.* **1992**, *96*, 5296−5302.
(12) Cattarin, S. *J. Appl. Electrochem.* **1992**, *22*, 1077−1081.
(13) Bouzek, K.; Paidar, M.; Sadilkova, A.; Bergmann, H. *J. Appl. Electrochem.* **2001**, *31*, 1185−1193.
(14) Macova, Z.; Bouzek, K. *J. Appl. Electrochem.* **2005**, *35*, 1203−1211.
(15) Simpson, B. K.; Johnson, D. C. *Electroanalysis* **2004**, *16*, 532−538.
(16) Sastry, K. V. H.; Moudgal, R. P.; Mohan, J.; Tyagi, J. S.; Rao, G. S. *Anal. Biochem.* **2002**, *306*, 79−82.
(17) Dima, G. E.; Beltramo, G. L.; Koper, M. T. M. *Electrochim. Acta* **2005**, *50*, 4318−4326.
(18) Delahay, P. *Double Layer and Electrode Kinetics*; Interscience Publishers: New York, 1965.
(19) Magnussen, O. M. *Chem. Rev.* **2002**, *102*, 679−725.

anion evinces a $c(2 \times 2)$ structure on Cu(100).[19] Sulfate forms a modified $(\sqrt{3} \times \sqrt{7})$ adlattice on Cu(111)[20] but not on Cu(100).[21] Oxoanion adsorption on metal electrodes always involves water or hydronium coadsorption.[22] The water or hydronium ion can form hydrogen-bridge bonds through the lone electron pairs of oxygen atoms which stabilize the observed structures.

Despite the large amount of literature examining electrode surface adsorption of many oxoanions,[19] there is only a sparse amount of literature examining nitrate or nitrite adsorption on metal electrode surfaces. In this context, FTIR measurements suggest that nitrate adsorbs in what is likely a twofold coordination geometry on Au.[8,10] The geometry adopted by nitrate on any Cu surface is unknown.

In this paper, we address the structure of adsorbed nitrate and intermediates as well as insight for nitrate reduction on the Cu(100) surface by using conventional electrochemical methods, in situ electrochemical scanning tunneling microscopy (EC-STM), surface enhanced Raman spectroscopy (SERS), and density functional theory (DFT) calculations.

2. Experimental Details

Solutions used in this work were prepared from ultrapure nitric acid (J. T. Baker) or sodium nitrite (Aldrich, 99.999%). The electrolytes were made from ultrapure $HClO_4$ (J. T. Baker) or HF (J. T. Baker) by using Milli-Q water (18.2 MΩcm, Millipore Inc.).

A 10 mm diameter Cu(100) single crystal (Monocrystals Co.) was polished to a mirror finish with 9, 3, 1, and 0.25 μm diamond suspensions, sequentially. The crystal was then electropolished in concentrated phosphoric acid,[23] rinsed with copious Milli-Q water, and immediately covered with the electrolyte solutions.

Cyclic voltammetric (CV) data were obtained in a two-compartment, glass electrochemical cell as previously reported.[24] The copper crystal was placed in the cell in a hanging meniscus configuration. The solutions were purged with Ar prior to use, and an Ar atmosphere was maintained in the cell during all electrochemical measurements. Rotating disk electrode (RDE) data were obtained using a Pine model MSRX rotator equipped with a Kel-F collet to hold the copper crystal. Scan rates for CV and RDE measurements were 50 mV/s and 4 mV/s, respectively.

EC-STM measurements were carried out using a Nanoscope III E (Digital Instrument Corp.) equipped with a fluid cell. The electropolished crystal was clamped to the bottom of the cell using an O-ring. Platinum wires were used for both the reference and counter electrodes. All potentials are reported with respect to the Ag|AgCl reference electrode for convenience. EC-STM tips were prepared by electrochemical etching of a tungsten wire (0.25 mm in diameter) in 2 M NaOH, followed by insulation with Apiezon Wax in order to reduce the area in contact with the electrolyte. This procedure minimized Faradaic current at the tip.

Before each SERS experiment, the mechanically polished Cu(poly) was electrochemically roughened by anodic dissolution at 0.5 V for 40 s and subsequent reduction at −0.8 V for 10 s in 0.2 M $CuSO_4$ + 0.4 M H_2SO_4 solution as reported.[25] SERS experiments were done at room temperature using an in situ cell described previously.[26] A HeNe laser (632.8 nm) was projected onto the sample at 45°. A 1200 grooves/nm grating dispersed radiation onto a cooled CCD (Andor). Typical acquisition time was 2 min. The system was allowed to equilibrate for 2 min at each potential before spectra were acquired.

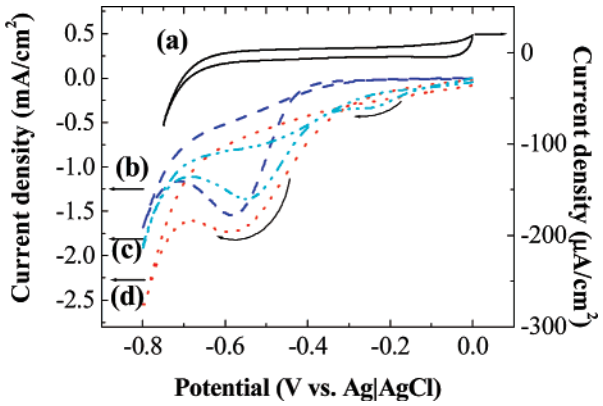

Figure 1. Cyclic voltammograms obtained from Cu(100) (a, b, and c) or Cu(poly) (d) surfaces in 0.1 M $HClO_4$ with addition of (a) nothing further, (b) 1 mM HNO_3, (c) 1 mM $NaNO_2$, and (d) 1 mM HNO_3.

Calculations on periodic structures were carried out using the Cambridge serial total energy package (CASTEP) in MSI-Cerius2.[27] Density functional theory (DFT) calculations with the generalized gradient approximation with the functional of Perdew and Wang (GGA-PW91) were performed.[28] Ultrasoft pseudopotentials were used to describe the electron−core interactions of Cu, O, and N. Valence states include the 3d and 4s shells for Cu and 2s and 2p for O and N. The electronic wave functions were expanded in a plane wave basis set with an energy cutoff of 400 eV. For the total energy calculations a Monkhorst−Pack *k*-point sampling scheme with 16 *k*-points for Cu(100) supercells. In this work, Cu(100) surfaces were modeled by a (2 × 2) unit cell consisting of three layers. The vacuum region between slabs was 10 Å. In all cases, surface modifications were applied only to one face of the slab. For NO_3 and NO_2 adsorption on the Cu surfaces, the topmost copper layer was allowed to relax during the adsorption process, whereas the other atoms in the bottom two layers were constrained in their position to mimic the bulk crystal. Calculations were performed using an SGI Origin 2000 computer within the School of Chemical Sciences at the University of Illinois.

3. Results

3.1. Cyclic Voltammetry. Figure 1 shows cyclic voltammograms (CVs) of the Cu(100) and Cu(poly) surface immersed in 0.1 M $HClO_4$ solutions without and with 1 mM HNO_3 or $NaNO_2$. In curve (a), a CV of Cu(100) obtained in 0.1 M $HClO_4$, the cathodic peak, which is associated with the hydrogen evolution reaction (HER), starts to increase at ca. −0.6 V. Between ca. −0.1 and −0.6 V, a featureless double layer region is observed. This CV is consistent with the Cu(100) voltammogram obtained previously.[21,29]

Curve (b) also shows the CV of Cu(100) obtained in a solution containing 0.1 M $HClO_4$ + 1 mM HNO_3. Between 0.0 and −0.3 V, a featureless flat region is observed. As the applied potential is moved to negative values, the cathodic current begins to increase around −0.3 V vs Ag|AgCl. The cathodic current

(20) Wilms, M.; Broekmann, P.; Stuhlmann, C.; Wandelt, K. *Surf. Sci.* **1998**, *416*, 121−140.
(21) Vogt, M. R.; Lachenwitzer, A.; Magnussen, O. M.; Behm, R. J. *Surf. Sci.* **1998**, *399*, 49−69.
(22) Kleinert, M.; Cuesta, A.; Kibler, L. A.; Kolb, D. M. *Surf. Sci.* **1999**, *430*, L521−L526.
(23) Cruickshank, B. J.; Sneddon, D. D.; Gewirth, A. A. *Surf. Sci.* **1993**, *281*, L308−L314.
(24) Schultz, Z. D.; Shaw, S. K.; Gewirth, A. A. *J. Am. Chem. Soc.* **2005**, *127*, 15916−15922.
(25) Zawada, K.; Bukowska, J. *Electrochim. Acta* **2004**, *49*, 469−476.
(26) Biggin, M. E. Ph.D. Thesis, University of Illinois at Urbana-Champaign, 2001.
(27) Milman, V.; Winkler, B.; White, J. A.; Pickard, C. J.; Payne, M. C.; Akhmatskaya, E. V.; Nobes, R. H. *Int. J. Quantum Chem.* **2000**, *77*, 895−910.
(28) Perdew, J. P.; Chevary, J. A.; Vosko, S. H.; Jackson, K. A.; Pederson, M. R.; Singh, D. J.; Fiolhais, C. *Phys. Rev. B* **1992**, *46*, 6671−87.
(29) Bae, S.-E.; Gewirth, A. A. *Langmuir* **2006**, *22*, 10315−10321.

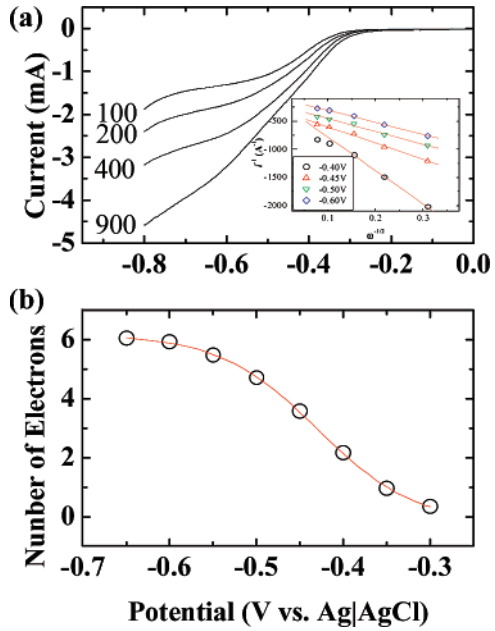

Figure 2. (a) Rotating disk electrode voltammograms obtained from Cu-(100) in 0.1 M $HClO_4$ + 1 mM HNO_3 solution. The numbers on left of the voltammograms denote the rotation rate (rpm), and the scan rate was 4 mV/s. The inset shows the Koutecky−Levich plots obtained at different electrode potentials. (b) The number of the electrons involved in the reduction as a function of applied potential was obtained from the Koutecky−Levich plots.

exhibits a peak at −0.58 V. The onset of the HER occurs at −0.72 V. There is no corresponding anodic current seen on the positive potential sweep, which means that the reduction of nitrate on the copper surface is irreversible. The CV shows a crossover feature at ca. −0.4 V ascribed to reduction of nitrite retained near the electrode after the negative potential excursion.[7]

Curve (c) shows the CV obtained from a Cu(100) crystal immersed in a solution containing 0.1 M $HClO_4$ + 1 mM $NaNO_2$. In contrast to the NO_3^- case, the cathodic current begins at 0.0 V and increases gradually as the potential is swept negatively. Around −0.2 V, a broad peak is observed which is associated with nitrite reduction.[7] The main reduction currents start to increase abruptly at −0.3 V and exhibits a peak at −0.53 V. The HER takes place at the same potential as that in the nitrate case.

Curve (b) shows the CV obtained from a Cu(poly) crystal immersed in a solution containing 0.1 M $HClO_4$ + 1 mM HNO_3. In contrast to the Cu(100) case, this CV shows cathodic current starting at 0.0 V. The reduction peak at −0.58 V is somewhat broader than that seen on the Cu(100) crystal. The CV in curve (d) also shows the crossover feature at −0.3 V, likely due to the same reason as that discussed for Cu(100). The voltammetry from Cu(poly) agrees well that reported earlier.[30]

3.2. Rotating Disk Electrode Measurements. Figure 2 shows RDE voltammograms obtained from a Cu(100) surface in a solution containing 1 mM HNO_3 + 0.1 M $HClO_4$ purged with Ar. The nitrate reduction current begins around −0.3 V, consistent with the cyclic voltammetry. To obtain the number of electrons associated with the nitrate reduction process on the Cu(100) surface in 0.1 M $HClO_4$ solution, the Koutecky−Levich plot was obtained and is shown in the inset. For each electrode

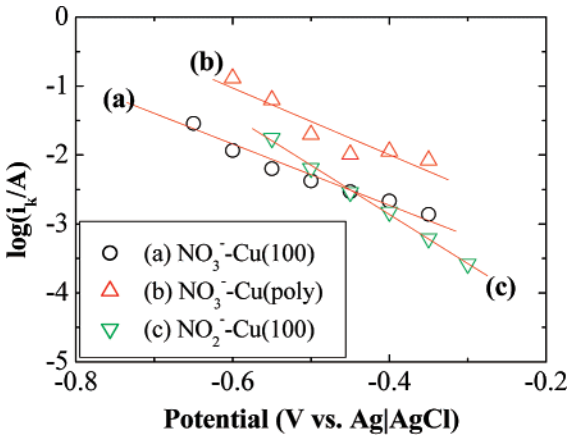

Figure 3. Tafel plots for Cu(100) (a and c) and Cu(poly) (b) in 0.1 M $HClO_4$ + 1 mM HNO_3 (a and b) or 1 mM HNO_2 (c).

potential, the inverse of the current, $1/i$, has a linear relationship with the inverse square root of the rotation rate, $\omega^{-1/2}$, according to the Koutecky−Levich equation;[31]

$$\frac{1}{i} = \frac{1}{i_k} + \frac{1}{0.62nFAD_0^{2/3}\omega^{1/2}\nu^{-1/6}C_0} \qquad (2)$$

where i_k is the limiting current, n is the number of electrons exchanged in the nitrate reduction reaction, F is the Faraday constant, A is the electrode area; D_0 is the diffusion coefficient of the nitrate (1.80×10^{-5} cm^{-1} s^{-1}),[5] ω is the rotation rate, ν is the kinematic viscosity (0.0088 cm^2 s^{-1}), and C_0 is the bulk concentration of the nitrate (1.0×10^{-6} mol cm^{-3}). By fitting the data in Figure 2a, the n value can be evaluated from the slope for each electrode potential. The n value (Figure 2b) ranges from 2 (−0.4 V) to 6 (−0.6 V) and slightly increases at more negative potentials. These n values suggest that nitrate reduction on the Cu(100) surface in 0.1 M $HClO_4$ is a six-electron process at negative potentials interrogated here. A similar analysis for Cu(poly) (Supporting Information) gave n = 8 in the same potential region, consistent with previous reports.[5]

The Tafel behavior for nitrate or nitrite reduction (Figure 3) was calculated using the RDE data reported above. The Tafel slopes were found to be 225, 139, and 206 mV/decade for nitrate, nitrite on Cu(100), and nitrate on Cu(poly), respectively. The slope obtained from the Cu(poly) surface in 0.1 M $HClO_4$ is identical with the value (203 mV/decade) for this reaction reported previously.[4] Additionally we measured exchange current densities from the Tafel plot for each reaction. The values are 56, 2.5, and 149 $\mu A/cm^2$ for nitrate, nitrite on Cu-(100), and nitrate on Cu(poly), respectively.

3.3. In Situ EC-STM. Figure 4 shows in situ EC-STM images of a Cu(100) surface obtained in 0.1 M HF without (a and b) and with (c and d) the presence of NO_3^-. In situ EC-STM measurements were obtained using HF electrolyte in order to minimize the presence of contaminants, such as Cl^-, which can decorate the bare Cu surface. The CVs obtained with 0.1 M HF supporting electrolyte were identical to those reported in Figure 1. The image shown in Figure 4a, obtained without NO_3^- at a potential of −0.3 V vs Ag/AgCl, exhibits wide meandering terraces and steps, and the high-resolution image

(30) Fogg, A. G.; Scullion, S. P.; Edmonds, T. E.; Birch, B. J. *Analyst* **1991**, *116*, 573−579.

(31) Bard, A. J.; Faulkner, L. R. *Electrochemical Methods*, 2 ed.; John Wiley & Sons: New York, 2001.

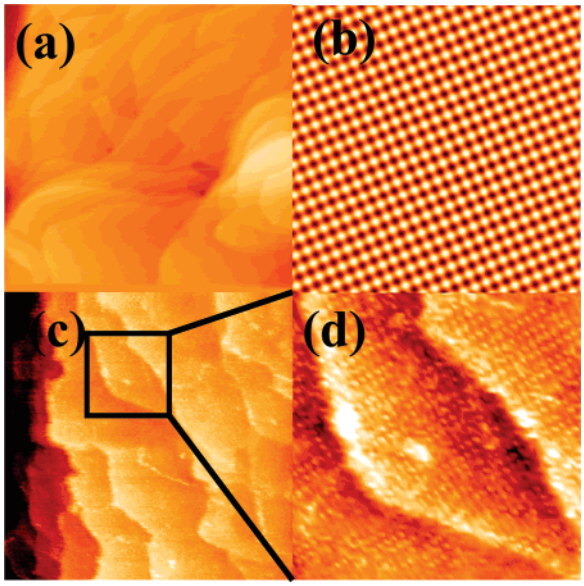

Figure 4. In situ EC-STM images of the Cu(100) surface obtained in 0.1 M HF. (a and b) were obtained in NO_3^--free solution while (c and d) were obtained in 1 mM HNO_3. (a and c) are large scale images (200 nm × 200 nm (a) and 50 nm × 50 nm (c)). (b and d) are smaller scale images (5 nm × 5 nm (b) and 16 nm × 16 nm (d)). The applied potentials are −0.3 V (a and b) and −0.03 V (c and d) for the electrodes and −0.25 V (a), −0.29 V (b), and −0.08 V (c and d) for the tips (all potentials reported vs Ag/AgCl). The tunneling currents are 2 nA (a), 18 nA (b), and 50 nA (c and d).

(Figure 4b) (filtered by 2D Fast Fourier Transform (FFT)) shows atomic distances of 0.26 ± 0.03 nm along with the expected square structure.

Figure 4c is an in situ STM image obtained at the open-circuit potential (OCP, ca. 0.03 V vs Ag/AgCl) immediately following addition of HNO_3 to give a final nitrate concentration of 1 mM. The image exhibits terraces and steps similar to those seen for the case of absent nitrate. Additionally, close inspection (Figure 4d) reveals the presence of small molecular-scale spots which can be seen on all of the terraces. These spots, shown in Figure 4d, exhibit a square adlayer with spot−spot distances equal to 0.52 ± 0.03 nm. The adlayer is aligned with the {110} directions, which means that the adlayer on the Cu(100) surface has a (2 × 2) structure. Additionally, the step edges are covered with white features with a height of 0.2 ± 0.05 nm. This is close to the Cu(100) monatomic step height leading us to speculate that the white features result from cuprous or cupric ions dissolved from step edges.

Figure 5a and b show in situ EC-STM images of the Cu-(100) surface in a solution containing 1 mM HNO_3 + 0.1 M HF obtained at −220 mV. The large scale image (Figure 5a) reveals that the surface is covered fully with the (2 × 2) adlayer, as the spacing and direction of the spots are identical with those reported in Figure 4d. The molecular scale image (Figure 5b) reveals that the (2 × 2) adlayer is complicated in that four large spots make up the unit cell (one of which, is marked with an outline), with two smaller spots, denoted by an arrow in Figure 5b, along one of the edges. The distance between the big spots is 0.52 ± 0.03 nm, and the distance between the small spot and the big one is 0.26 ± 0.02 nm. Corrugations show 0.09 ± 0.02 nm for big spots and 0.08 ± 0.02 nm for small spots. The lattice is aligned with the {110} directions.

We carried out in situ EC-STM of Cu(100) in NO_2^--containing solution in order to compare NO_3^- and NO_2^-

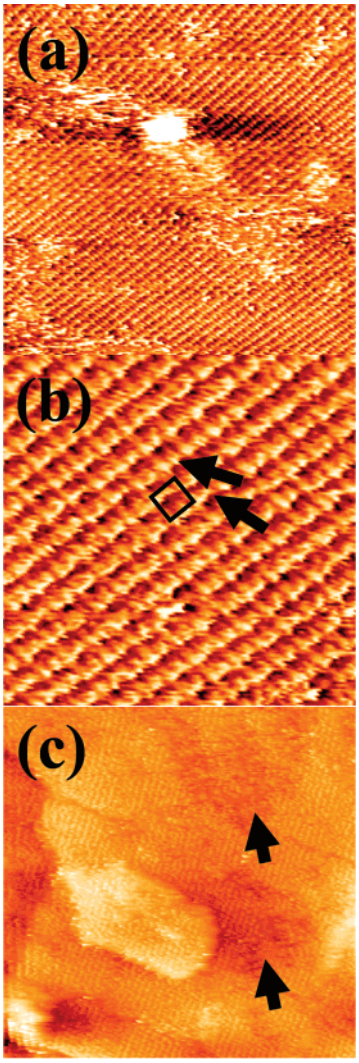

Figure 5. In situ EC-STM images of the Cu(100) surface were obtained in 1 mM HNO_3 + 0.1 M HF (a and b) or in 1 mM $NaNO_2$ + 0.1 M HF (c). The applied potentials are −0.22 V (a and b) and 0.0 V (c) for the electrodes and −0.25 V (a and b) and −0.05 V (c) for the tips. The tunneling currents are 20 nA (a and b) and 4 nA (c). Image sizes are 18 nm × 18 nm (a and c) and 7 nm × 7 nm (b).

adlayers. Figure 5c shows an in situ EC-STM image obtained from a 0.1 M HF solution containing 1 mM NO_2^-. This image was obtained at OCP (ca. 0.0 V vs Ag/AgCl). The image shown in Figure 5c exhibits a square lattice with atomic distances of 0.36 ± 0.04 nm. This lattice is rotated by 45° relative to the NO_2-free system which means that the adlattice of NO_2^- on Cu(100) exhibits a $c(2 \times 2)$ structure. Arrows in Figure 5c indicate areas which evince a rough and nonflat surface. Separate electrochemical measurements showed that an electrochemical reaction occurs on the W tips in NO_2^--containing solution at nearly all accessible potentials which made continued scanning in this solution problematic. This tip reaction was not found in solutions containing NO_3^-.

Figure 6 shows in situ EC-STM images obtained in a solution containing 0.1 M HF + 1 mM NO_3^- taken immediately after the potential was stepped from −220 mV to −250 mV vs Ag|AgCl. At this potential the well-defined spots observed in Figure 5b became disordered and could not be easily observed. However, the rows in Figure 6a are still oriented in the {110} direction. The arrow in the upper right corner of Figure 6a shows

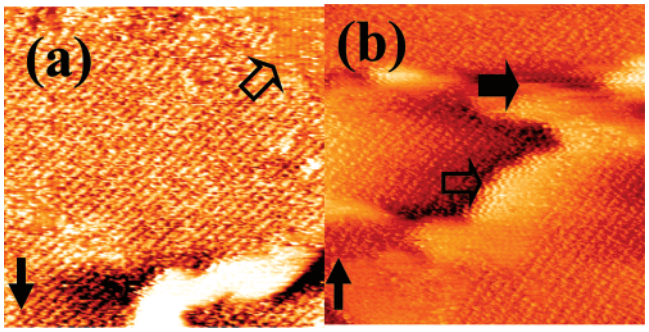

Figure 6. In situ EC-STM images of the Cu(100) surface were obtained in 1 mM HNO_3 + 0.1 M HF at −0.25 V. (a) shows a flat area while (b) reveals a step site. (b) was obtained 39 s following the acquisition of the image in (a). Image size is 18 nm × 18 nm. Tip potential and tunneling current are −0.28 V and 30 nA, respectively.

the initial stages of a new adlayer forming on this surface, the structure of which will be discussed below.

Figure 6b shows an in situ EC-STM image obtained under the same conditions as those for Figure 6a. The step marked with the open arrow in Figure 6b is well resolved and does not evince the frizzy behavior seen in other contexts.[32] However, the steps marked with closed arrows do exhibit the frizzy behavior. The step height is 0.18 nm consistent with a monoatomic step on the Cu(100) surface. The frizzy step is oriented in the {100} direction, which means that a (110) face is exposed. Interestingly, although most of the terrace region exhibits the (2 × 2) adlattice, the area immediately to the right of the open area shows a different adlattice structure, which is identical with that growing in the upper right of Figure 6a.

At slightly more negative potentials the new adlayer found in Figure 6 becomes more prominent. Figure 7 shows in situ EC-STM images obtained at −290 mV. In Figure 7a, the (2 × 2) adlattice is seen in a few positions of the image. At the upper middle position a new adlattice, rotated 45° relative to the (2 × 2) structure, is present. This adlayer exhibits spot−spot distances of 0.36 ± 0.03 nm. The new adlayer is thus a $c(2 \times 2)$ structure on the Cu(100) surface. The arrows in Figure 7a indicate protruded spots. The protrusions are located on random positions and especially on the boundary between the (2 × 2) and $c(2 \times 2)$ structures. Figure 7b shows a cross section obtained along the line drawn in Figure 7a. The protrusion height is 0.2 ± 0.05 nm which is higher than a normal adlayer and close to the Cu(100) monatomic step height. The line drawn in Figure 7a is located exactly over the (2 × 2) spots and along the {100} direction. It also crosses over the $c(2 \times 2)$ spots with a 45° rotation.

Figure 7c shows an in situ EC-STM image obtained at −290 mV 13 s after the acquisition of the image in Figure 7a. The new $c(2 \times 2)$ layer gradually expands the area while the (2 × 2) area becomes narrow simultaneously. Figure 7d shows a STM image obtained at −330 mV. At this potential, the $c(2 \times 2)$ structure dominates on the surface and relatively little (2 × 2) structure remains.

Figure 8 shows in situ EC-STM images obtained at more negative potentials. Figure 8a shows an in situ EC-STM image obtained at −0.47 V. A number of defects are formed throughout the entire surface, which means that the adlayer formed at more

(32) Giessen, H.; Butty, J.; Woggon, U.; Fluegel, B.; Mohs, G.; Hu, Y. Z.; Koch, S. W. *Phase Transitions* **1999**, *68*, 59−94.

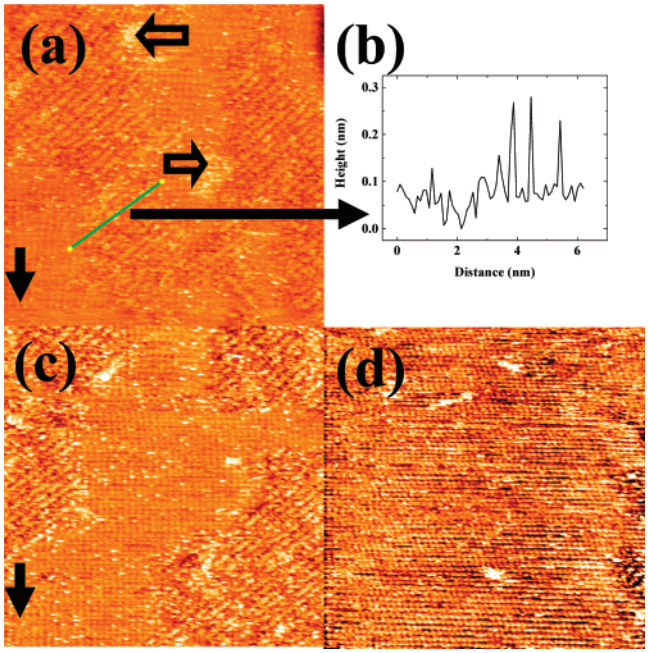

Figure 7. In situ EC-STM images (a, c, and d) and cross section (b) of the Cu(100) surface were obtained in 1 mM HNO_3 + 0.1 M HF at −0.29 V (a, b, and c) and −0.33 V (d). (c) was obtained after 13 s after (a). Image size is 18 nm × 18 nm. The tip potentials are −0.31 V (a and b) and −0.36 V (d). The tunneling current is 30 nA.

positive potentials is changing. The depth of the defects is typically 0.06 ± 0.02 nm. The angles formed by the defects are 90° and 70°. The former is along the {110} direction. While the adlayer structure, if it exists, in the defect rows is not resolved, the structure of the adlayer around the defects is readily seen. The distance between spots in the raised adlayer is 0.52 nm. Arrow A indicates the spots which are round and symmetric. Arrow B indicates the spots aligned along the {100} direction that are small and distorted. These might result from splitting of the round spots.

Figure 8b and 8c show in situ EC-STM images obtained in the same solution as that used for Figure 8a at −0.53 V. The images show that the nascent adlayer forming in Figure 8a has now grown to nearly cover the entire surface. In Figure 8b, some defects remain, such as that marked by arrow C, but these are absent in Figure 8c. High-resolution images of the adlayer still occasionally reveal the 0.52 nm spot−spot spacing detailed above. However, the spots do not appear ordered, and no assignment of adlayer structure can be made. All steps in Figure 8 show the "frizzy" behavior, indicative of adatom or admolecule movement along the step edge. Table 1 provides a summary of the structures observed by in situ STM during the measurements performed here.

3.4. SERS Measurements. In order to provide further insight into the mechanism of nitrate reduction, SERS was used to investigate the species on the surface during the nitrate reduction process. The SER spectra were recorded at Raman shifts between 450 and 1680 cm^{-1}. Table 2 gives all the peaks observed and their assignments.

Figure 9a shows the SER spectra obtained from Cu(poly) in a solution containing 0.1 M $HClO_4$ + 0.5 mM HNO_3 in the absence of oxygen. The main features are a sharp peak at 933 cm^{-1} which is attributed to the symmetric Cl−O stretch of perchlorate (peak A), a peak at 972 cm^{-1} (peak B) associated

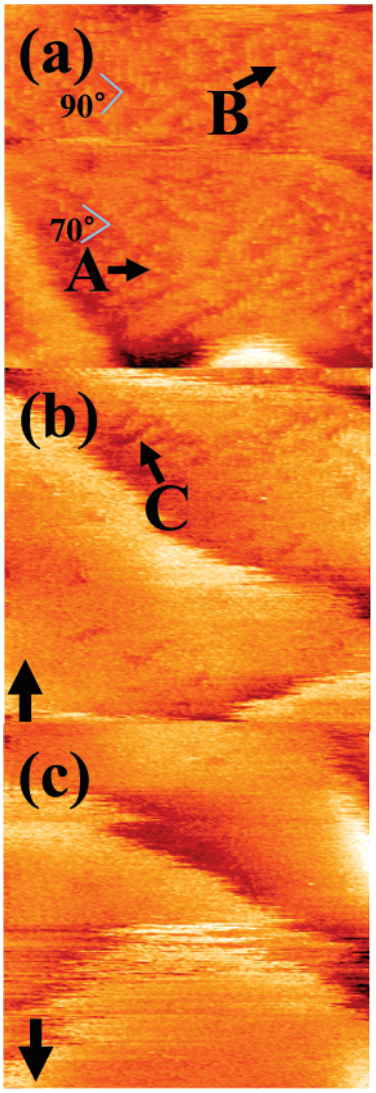

Figure 8. In situ EC-STM images of the Cu(100) surface were obtained in 1 mM HNO_3 + 0.1 M HF at −0.47 V (a) and −0.53 V (b and c). (b and c) were obtained sequentially. Image size is 18 nm × 18 nm. Tip potential and tunneling current are −0.50 V and 30 nA, respectively.

with $Cu(SO_4)$ used in the roughening process, and two broad peaks centered at 1346 cm^{-1} (peak C) and 1610 cm^{-1} (peak D). Peak C at 1346 cm^{-1} is assigned to a doubly degenerate stretching mode of NO_3^- consistent with the transmittance spectra of 1 M HNO_3 aqueous solution.[10] Peak D at 1610 cm^{-1} is attributed to the bending of water molecules.[33] Band E at 1370 cm^{-1} can be assigned to metal NO_3^- complexes and is found in the Raman and IR spectrum.[34,35] In the spectral region around 625 cm^{-1}, peak G assigned to the Cu−O stretch of Cu_2O is observed.[36] Band F at 850 cm^{-1} and band H at 1240 cm^{-1} are attributed to the bending mode and symmetric stretching of nitrite ions.[10,34] The band H persists until −0.45 V and then disappeared at −0.55 V.

Independent SERS measurement (Figure 9b) obtained from a Cu(poly) surface immersed in a solution containing 0.1 M HF + 10 mM $NaNO_2$ confirm the presence of nitrite following nitrate addition reported in Figure 9a. The spectrum in Figure 9b shows two peaks at 1240 cm^{-1} (peak H′) and 1389 cm^{-1} (peak I) characteristic of nitrite. Peak H′ and peak I are attributed to symmetric and antisymmetric N−O stretches of nitrite, respectively.[10] Additionally the spectrum reveals bands at 520 cm^{-1} (peak J), 609 cm^{-1} (peak K), 638 cm^{-1} (peak L), and 850 cm^{-1} (peak F′). The Cu_2O peaks are typically found in the region around 525 cm^{-1} and 613−653 cm^{-1}.[36−42] A shoulder occurs at 520 cm^{-1} (peak J) while the peak around the region 613−653 cm^{-1} is divided by two as peaks K and L. Nonetheless, finding the peaks in the two regions suggests that Bands J, K, and L are associated with Cu_2O. Interestingly a vestige (peak F′) of a feature at 850 cm^{-1} is seen in Figure 8a. Table 2 provides a summary of the assignments for peaks observed by SERS during the measurements performed here.

Figure 10 shows the potential dependence of the relative SERS intensity from peak H (nitrite) and E (nitrate) in nitrate-containing solution, along with the behavior of peak H′ in nitrite solution. The relative intensity of peak H obtained in nitrate-containing solution declines slightly from +0.05 V to −0.15 V, increases abruptly around −0.2 V, and declines at −0.5 V. The intensity of peak E, associated with the NO_2 antisymmetric stretch of nitrate, is relatively constant until reaching ca. −0.3 V where it begins to decline. The intensity of peak H′ obtained in the nitrite containing solution declines rapidly as the potential is moved negative from OCP.

3.5. DFT Calculations. To further understand the interaction between Cu surfaces, nitrate, and nitrite, we performed DFT calculations. The interaction of NO_3^- and NO_2^- with an fcc metal surface has not been yet reported. Calculation for bare Cu(100) revealed a lattice spacing = 0.353 nm and a surface energy = 0.096 eV/Å^2, in close accord with the experimental values of 0.362 nm and 0.112 eV/Å^2, respectively.[43]

In order to model nitrate or nitrite association with Cu(100), we performed calculations interacting neutral NO_3 or NO_2 with the (2 × 2) Cu(100) slab. We used the neutral species as a starting point for our calculations, with the intent of examining the degree of charge transfer from the surface to the molecular species.

Table 3 shows the results of these calculations, while Figure 11 shows the optimized geometry for both nitrate and nitrite adsorption on Cu(100). Both molecules are adsorbed on the bridge sites of the Cu(100) surface through two oxygen atoms. The calculations also show that the interaction between the ions and Cu are quite strong, with $\Delta E_{ads} = -2.582$ eV for nitrate ion and −1.964 eV for nitrite ions. These values are higher than those found experimentally for nitrate adsorbed onto the $Pd_{0.78}/Cu_{0.22}$ bimetallic surface (−0.23 eV)[44] and computationally for methyl nitrite on Au(111) (−0.35 eV).[45] Cu is one of

(33) Oda, I.; Ogasawara, H.; Ito, M. *Langmuir* **1996**, *12*, 1094−1097.
(34) Irish, D. E.; Brooker, M. H. *Advances in Infrared and Raman Spectroscopy*; Heyden: London, 1976.
(35) Castro, P. M.; Jagodzinski, P. W. *Spectrochim. Acta, Part A* **1991**, *47*, 1707−1720.
(36) Chan, H. Y. H.; Takoudis, C. G.; Weaver, M. J. *J. Phys. Chem. B* **1999**, *103*, 357−365.
(37) Hamilton, J. C.; Farmer, J. C.; Anderson, R. J. *J. Electrochem. Soc.* **1986**, *133*, 739−45.
(38) Baddorf, A. P.; Wendelken, J. F. *Surf. Sci.* **1991**, *256*, 264−71.
(39) Heltemes, E. C. *Phys. Rev.* **1966**, *141*, 803−5.
(40) McDevitt, N. T.; Baun, W. L. *Spectrochim. Acta* **1964**, *20*, 799−808.
(41) Melendres, C. A.; Xu, S.; Tani, B. *J. Electroanal. Chem.* **1984**, *162*, 343−9.
(42) Sullivan, D. H.; Conner, W. C.; Harold, M. P. *Appl. Spectrosc.* **1992**, *46*, 811−18.
(43) Lide, D. R.; Frederikse, H. I. R. *CRC Handbook of Chemistry and Physics*, 76th ed.; CRC Press: New York, 1996.
(44) Pintar, A.; Batista, J.; Levec, J.; Kajiuchi, T. *Appl. Catal., B* **1996**, *11*, 81−98.
(45) Gomes, J. R. B.; Illas, F. *Catal. Lett.* **2001**, *71*, 31−35.

Table 1. Structural Parameters of Nitrate Reductions for Cu(100) at Different Potentials in Nitric Acid Solution

applied potential ranges vs Ag|AgCl	main structure	atomic distance (nm)	corrugation (nm)	steps	assignments
all range without nitrate	(1 × 1)	0.26	<0.01	frizzy, rounded	Cu(100)
OCP to −0.33 V	(2 × 2)	0.52	0.09	noisy, rounded	NO_3
−0.25 V to −0.47 V	c(2 × 2) and (2 × 2)	0.52 and 0.36	0.09 and 0.04	frizzy in (110) face, rounded	NO_3 or NO_2
−0.47 V to	disordered	--	--	frizzy, rounded	unknown

Table 2. Experimentally Observed Raman Peaks and Assignments

peak label	SERS nitrate solution	SERS nitrite solution	assignment
A	933	-	Cl-O stretch
B	972	-	S−O stretch
C	1346	-	NO_2 of NO_3^- symmetric stretch
D	1610	-	H_2O bending
E	1370	-	NO_2 of NO_3^- antisymmetric stretch
F	625	-	Cu−O stretch
G	850	850	NO_2 bending
H	1240	1240	NO_2^- symmetric stretch
I	-	1389	NO_2^- antisymmetric stretch
J, K, L	-	520, 609, 638	Cu_2O

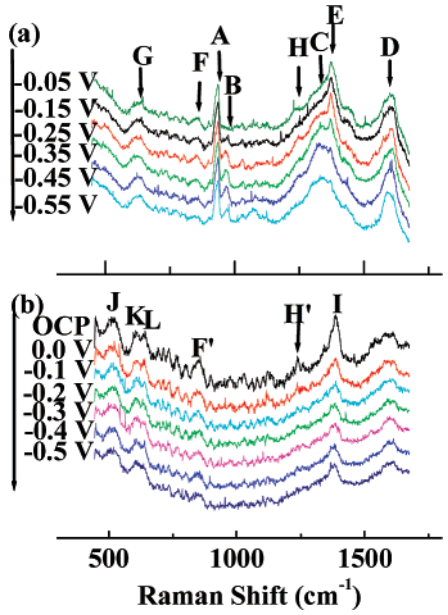

Figure 9. SER spectra from Cu(poly) + 0.1 M $HClO_4$ + 0.5 mM HNO_3 (a) and Cu(poly) + 0.1 M HF + 10 mM HNO_2 (b) in Ar atmosphere. The cathodic sweep is shown.

the most oxophilic metals,[46] so an increase in stabilization is anticipated.

Additionally, the calculations show that the nitrate and nitrite produce other changes in the Cu surface. The Cu−O distances for both molecule calculations are found to be approximately 0.196 nm, which is the same as the Cu−O distance found in CuO (0.196 nm), indicating the formation of a Cu−O bond. Interestingly, the N−O bonds are elongated relative to free nitrate or nitrite molecules: from 0.126 nm to 0.130 for the nitrate and from 0.122 to 0.127 nm for the nitrite. The Mulliken population charge on the NO_3 molecule is −0.58 e, indicating

(46) Koper, M. T. M.; van Santen, R. A. *J. Electroanal. Chem.* **1999**, *472*, 126−136.

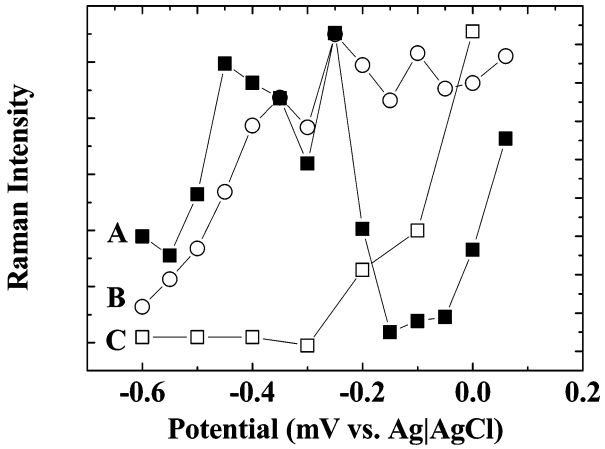

Figure 10. Potential dependence of SER spectra intensity obtained from Cu(poly) in acidic nitrate (A and B) or nitrite solutions (C). (A) is obtained from Band H (nitrite) at 1240 cm^{-1}, and (B) is obtained from band E (nitrate) at 1370 cm^{-1} in Figure 9a. (C) is obtained from Band H′ (nitrite) at 1240 cm^{-1} in Figure 9b.

that the molecule adopts some anionic character following surface interaction. By way of comparison the charge on the NO_2 molecule is −0.42 e. The surface Cu atoms are oxidized by nearly 0.25 e for nitrate and 0.13 e for nitrite.

We also repeated the calculations imposing a −1 charge on the metal surface. This negative charge shifts the Fermi energy to more positive values, the magnitude of which is loosely associated with a corresponding change in electrode potential.[47] In both the nitrate and nitrite cases, the adsorption energy shows little difference with the zero charge case. However, in the nitrite case, the negative charge results in a smaller N−O bond length elongation relative to the zero charge case. The Cu−O bond distance increases in the −1 charge case relative to case of the zero charge, suggesting that the nitrate anion is less stable at the negative potential represented by the −1 charge relative to zero charge, as anticipated. A similar change is also found for the nitrite case.

4. Discussion

The results presented here provide considerable insight regarding the reduction of nitrate on Cu(100) surface. In particular, the results speak to structures formed by the reduction intermediates on the Cu(100) surface and to their temporal evolution. These observations provide insight into mechanisms of nitrate reduction on Cu(100).

4.1. Electrochemical Measurements. The CVs obtained from nitrate or nitrite solution exhibit somewhat different features from each other. The CV of the Cu(100) surface in nitrate solution shows a featureless double layer region until −0.3 V and a reduction current from −0.3 to −0.72 V with a

(47) Li, X.; Gewirth, A. A. *J. Am. Chem. Soc.* **2003**, *125*, 11674−11683.

Table 3. Comparison of Adsorption Energy and Geometric Properties of NO_3 and NO_2 on Cu(100) Surfaces

surface property	NO_3 on Cu(100) 0e	NO_2 on Cu(100) 0e	NO_3 on Cu(100) −1e	NO_2 on Cu(100) −1e
E_{Fermi} (eV)	0.477	0.432	1.011	1.051
ΔE_{Fermi}[a] (eV)	0.207	0.162	0.0127	0.0540
E_{ad}[b] (eV)	−2.58	−1.964	−2.58	−1.953
N−O[c] (Å)	1.230, 1.300, 1.300	1.269, 1.271	1.251, 1.287, 1.288	1.278, 1.279
O−M (Å)	1.972, 1.963	1.963, 1.976	2.055, 2.060	2.039, 2.053
ΔM[d] (Å)	−0.0054, −0.0058	0.001, −0.0013	−0.001, −0.006	−0.0038, −0.0023
q_M[e]	0.15, 0.10	0.07, 0.05	0.09, 0.09	0.03, 0.02
q_O	−0.40, −0.40, −0.30	−0.33, −0.34	−0.41, −0.41, −0.42	−0.38, −0.37
q_N	0.52	0.25	0.51	0.16

[a] ΔE_{Fermi} (eV) = $E_{Fermi}(NO_x/M) - E_{Fermi}(M)$. [b] $E_{ad} = E(NO_x/M) - E(NO_x) - E(M)$. [c] For free NO_x, the N−O bond is 1.256 Å, the calculated Mulliken charges are 0.67 for N and −0.22 or −0.23 for O. [d] The vertical shift distance of the metal atom which is directly interacting with O. [e] The calculated Mulliken charge of Cu atoms that are in close contact with O.

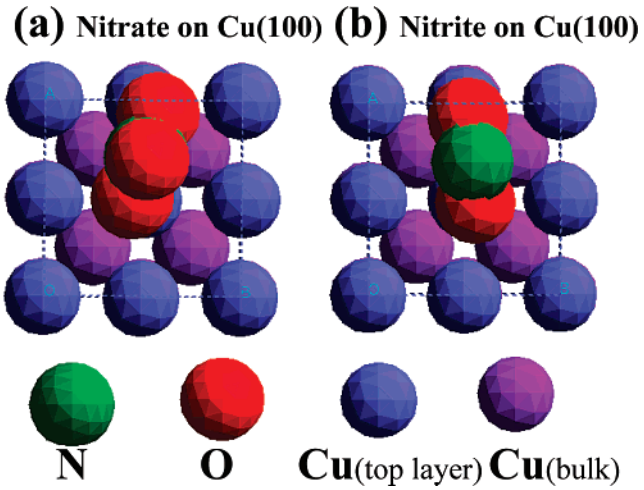

Figure 11. Illustration of nitrate (a) and nitrite (b) adsorption on Cu(100) surfaces.

peak at −0.58 V. In the case of the Cu(poly) surface in nitrate solution, a small reduction current was observed even close to the OCP and the main reduction current was observed in the same potential region as Cu(100). The difference could be attributable to the crystallinity of the surface. Polycrystalline Cu is known to dissolve spontaneously in an acidic nitrate solution at the OCP.[4,48] The low reduction current prior to the main nitrate potentials might result from the copper dissolution by nitrate ions in the acidic solutions.[4,48]

Between 0.0 and −0.15 V, observation and potential-dependent decrease of the nitrite band in SERS spectra suggest strongly that a nitrite ion is one of the products of this reduction. However, in situ EC-STM images show that the nitrate ion does not dissolve the Cu(100) surface. The coincident increase in reduction current between −0.15 and −0.5 V and the nitrite band at 1240 cm^{-1} suggest as well that nitrite is the main product in this potential region. At more negative potential than −0.5 V, the nitrite peak declines which suggests that the nitrite proceeds to a further reduction reaction. The CV obtained from the solution containing nitrite shows a broad peak around −0.25 V. Simultaneously, the band at 1240 cm^{-1} assigned to nitrite decreases and disappears. Thus the broad peak of the CV at −0.25 V is attributed to nitrite reduction,[7] while the main peak at −0.53 V is likely associated with further reduction of the products of the initial nitrite reduction.

Analysis of the RDE data reported above suggests that nitrate reduction is a six and eight electron process on Cu(100) and Cu(poly) at −0.6 V, respectively. Previous measurements for the nitrate reduction on a Cu(poly) surface in acid media found $n = 8$. The decreased value we report here for Cu(100) could arise from different sources. First, calculations of the n value require an accurate determination of surface area (A); a too large A will yield a small n value. In order to compare surface areas between Cu(poly) and Cu(100), we performed Pb underpotential deposition (upd) on both surfaces. From coulometry associated with the Pb upd, and by assuming the Pb upd process consumes two electrons per Pb atom,[49] we obtain the effective surface area. By using this method, we found that the effective area for our Cu(poly) sample was only 2.6% larger than that found for Cu(100). Thus, changes in surface area cannot be associated with the change in n value between the two electrodes.

The second possible origin of the different n values between Cu(poly) and Cu(100) may be attributed to different mechanistic pathways between the two surfaces. Interestingly, while corrosion behavior is apparent on the Cu(poly) surface (and is also found on Cu(111) (data not shown)), such is not the case on Cu(100), particularly at low overpotentials. The nitrate reduction exchange current density for Cu(poly) is also three times larger than the one for Cu(100). The observation of corrosion-like behavior on Cu(poly) suggests that either cuprous or cupric or both ions will be more abundant on the Cu(poly) surface relative to Cu(100). The cuprous ion is well-known to be a catalyst for nitrate reduction.[50] Interestingly, $n = 6$ was also observed on a Cu_x/Ni_{1-x} alloy material when $x \leq 0.5$.[15] This also suggests that limited Cu availability could contribute to different n values.

The image shown in Figure 6b shows that the Cu(110) face (formed at the step edge) is less stable than the Cu(100) terrace. The corroding Cu(110) face could therefore be a source of reactive cuprous ions. Indeed, analysis of Figure 6b shows that the terrace area to the right of the step edge is covered with a $c(2 \times 2)$ adlattice, indicating that the nitrate to nitrite reaction has occurred here. Cu availability occasioned by steps could be a source of the observed reactivity.

The Tafel slope obtained for nitrite reduction on Cu(100) (139 mV/decade) is roughly consistent with a one electron process as the rate determining step (rds) where a value of 118 mV/decade is expected.[18] Alternatively, for both Cu(100) and Cu(poly) the somewhat larger Tafel slope for nitrate reduction

(48) Schmid, G. *Z. Elektrochem.* **1959**, *63*, 1183.
(49) Brisard, G. M.; Zenati, E.; Gasteiger, H. A.; Markovic, N. M.; Ross, P. N. *Langmuir* **1995**, *11*, 2221−2230.
(50) Filimonov, E. V.; Shcherbakov, A. I. *Prot. Met.* **2004**, *40*, 280−284.

suggests that the rds is somewhat more involved. Interestingly, Dima et al.[4] reported that the first electron transfer is the rds for nitrate reduction on metal surfaces such as Ag, Pt, and Rh. Large (>120 mV/decade) Tafel slopes are typically interpreted as arising through a CE electrochemical mechanism, in which the chemical or C step is rate determining and the E or electrochemical step is fast.[18] The C step could be associated with production of cuprous ions. Alternatively, since relatively little corrosion behavior is observed on Cu(100) in STM images, another possibility might be activation of the NO bond on the Cu(100) surface.

4.2. Structures. EC-STM images obtained from nitrate free solutions exhibit an unreconstructed Cu(100) atomic structure which agrees fully with that reported previously.[21,51]

The CV of Cu(100) obtained from nitrate solution shows that the nitrate reduction begins around −0.3 V, consistent with the growth of the nitrite signal in the SERS spectra at these potentials. In the STM, the adlayer observed at potentials more positive than −0.3 V exhibits a (2 × 2) adlattice implying 25% surface coverage. In SERS spectra, we observe that the peak at 1370 cm^{-1} (nitrate) is dominant in this potential range. This suggests that the (2 × 2) adlattice in STM images is associated with a nitrate adlayer on Cu(100). We are aware that direct comparison between the STM on Cu(100) and the SERS obtained from Cu(poly) is complicated by the putative presence of different pathways (discussed above).

A number of papers report ordered sulfate or phosphate adlayers on fcc(111) or fcc(100) surfaces.[19,22,52−58] The adsorption of oxoanions always features coadsorption of water or a hydronium ion.[19,22] The water or hydronium ion can form hydrogen-bridge bonds through the lone electron pairs of oxygen atoms which apparently stabilizes the observed structures. On the basis of these previous studies, we propose that the nitrate adlayer on Cu(100) also incorporates the hydronium. The adlayer observed in the in situ EC-STM image of Figure 5b shows the two-spot motif typically found in these coadsorption adlayer systems. In this case, the distance between big spots is 0.52 nm, and that between the big and small spots is 0.26 nm. In the sulfate on Au(100) case, the corresponding distances are 0.4 and 0.28 nm, respectively. The presence of a water bending mode in the SERS suggests that water may be present on the electrode surface. Therefore, we suggest that the big spot is associated with the nitrate anion and the small spot is associated with hydronium. According to the calculations described above, the nitrate ion is adsorbed at the Cu(100) surface through two oxygen atoms. If the hydronium ions also are adsorbed on bridge sites, the distance between the oxygen of nitrate and the hydrogen of hydronium ions would be about 0.26 nm which is very close to the distance of the hydrogen bond (H-bond) (0.26 nm).[59] Figure 12a shows a model describing our proposed

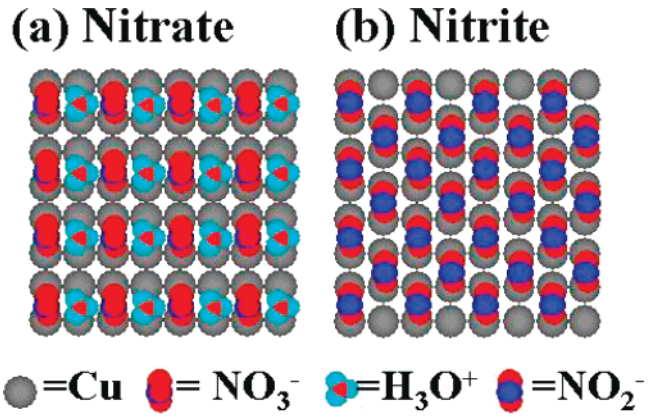

Figure 12. Schematic model of the nitrate (a) and nitrite (b) adlayer on the Cu(100) surface.

structure. The nitrate ions are placed on bridge sites of the Cu(100) surface. Every hydronium adsorbed on such a site can form the H-bond with the oxygen atoms of the neighboring nitrate ions.

As the applied potential decreases to lower than −0.3 V, we observe formation of a $c(2 \times 2)$ adlattice on the Cu(100) surface. Simultaneously, SERS data obtained from a solution containing nitrate exhibit a peak at 1240 cm^{-1} which is associated with nitrite. STM images obtained in nitrite alone also exhibit a $c(2 \times 2)$ adlattice. These observations suggest that the $c(2 \times 2)$ adlattice can be associated nitrite ions adsorbed on the Cu(100) surface. Interestingly, the nitrite adlattice appears to grow at the expense of the nitrate via a nucleation and growth mechanism, across the terraces. Both the cross sectional STM analysis and the calculations suggest that the nitrite ions are located at the same bridge sites of the Cu(100) surface that were found for nitrate. However, we never observed any intermediate spots which could be associated with water or hydronium coadsorption. We suggest that the more negative potential and possibly higher packing density may preclude this feature. Figure 12b is a model showing how nitrite ions may adsorb onto the Cu(100) surface.

When we applied a more negative potential (−0.37 V), the $c(2 \times 2)$ adlattice changes into a disordered structure. We could not extract additional information about this adlattice from SERS. Possibilities for this structure include (a) the adsorbed NO molecule, (b) another intermediate, such as NH_3, or (c) a bare Cu(100) surface. Among these, we favor possibility (a) for a few reasons. First, the further reduction of nitrite could yield NO, N_2O, NH_4OH, or NH_3. Since not all of these are soluble, it is likely that an intermediate species is still present on the Cu(100) surface. Among these molecules, N_2O and NH_4OH are too large to yield the structures observed on the Cu(100) surface. Second, the potential range in which the structure is obtained is not negative enough to produce NH_3. Thus we speculate that the disordered structure might be associated with a NO adlayer.

5. Conclusions

We examined the interaction between nitrate ion and Cu surfaces by using electrochemical measurements and in situ EC-STM, SERS, and DFT calculations. RDE results showed that the nitrate reduction is a six-electron process on the Cu(100) surface, while it is an eight-electron process on the Cu(poly)

(51) Vogt, M. R.; Moller, F. A.; Schilz, C. M.; Magnussen, O. M.; Behm, R. J. *Surf. Sci.* **1996**, *367*, L33−L41.
(52) Schweizer, M.; Kolb, D. M. *Surf. Sci.* **2003**, *544*, 93−102.
(53) Cuesta, A.; Kleinert, M.; Kolb, D. M. *PCCP* **2000**, *2*, 5684−5690.
(54) Ataka, K.; Osawa, M. *Langmuir* **1998**, *14*, 951−959.
(55) Ataka, K.; Yotsuyanagi, T.; Osawa, M. *J. Phys. Chem.* **1996**, *100*, 10664−10672.
(56) Lennartz, M.; Broekmann, P.; Arenz, M.; Stuhlmann, C.; Wandelt, K. *Surf. Sci.* **1999**, *442*, 215−222.
(57) Funtikov, A. M.; Linke, U.; Stimming, U.; Vogel, R. *Surf. Sci.* **1995**, *324*, L343−L348.
(58) Edens, G. J.; Gao, X. P.; Weaver, M. J. *J. Electroanal. Chem.* **1994**, *375*, 357−366.
(59) Clair, S.; Pons, S.; Seitsonen, A. P.; Brune, H.; Kern, K.; Barth, J. V. *J. Phys. Chem. B* **2004**, *108*, 14585−14590.

surface. Tafel slopes obtained on Cu surfaces were somewhat larger than 118 mV/decade, suggesting that nitrate reduction is not a simple one- or two-electron process but instead a CE mechanism is at play.

Additionally, in situ EC-STM and SERS measurements suggest that from the OCP to a potential of −0.3 V, the Cu(100) surface is covered with the nitrate molecules. Potential excursion to the potential region between −0.3 and −0.5 V yields a new structure, which we associate with adsorbed nitrite. The transition between the two adsorbates is observed and proceeds via a nucleation and growth mechanism. The presence of the adsorbed nitrite ions shows that it is an intermediate in the nitrate reduction. The nitrate forms a (2×2) adlattice while the nitrite ion exhibits a $c(2 \times 2)$ adlattice, the analysis of which suggests that a hydronium or some other species plays a role in its stabilization. DFT calculations suggest that both the nitrate and nitrite ions are adsorbed on bridge sites of the Cu(100) surface through two oxygen atoms.

Acknowledgment. S.E.B. acknowledges the Korea Research Foundation for a fellowship (No. KRF-2005-214-C00068). This work was funded by the NSF (CHE- 06-03675), which is gratefully acknowledged.

Supporting Information Available: Rotating disk electrode voltammograms and the Koutecky−Levich plots obtained for nitrate reduction on Cu(poly). This information is available free of charge via the Internet at http://pubs.acs.org.

JA071330N